THE JOURNAL OF BIOLOGICAL CHEMISTRY VOL. 290, NO. 26, pp. 16043–16058, June 26, 2015

Ganglioside GD3 Enhances Invasiveness of Gliomas by Forming a Complex with Platelet-derived Growth Factor Receptor α and Yes Kinase*

Received for publication, December 29, 2014, and in revised form, May 2, 2015 Published, JBC Papers in Press, May 4, 2015, DOI 10.1074/jbc.M114.635755

Yuki Ohkawa[‡§¶], Hiroyuki Momota[§], Akira Kato[§], Noboru Hashimoto[‡], Yusuke Tsuda[‡], Norihiro Kotani[‖], Koichi Honke[**], Akio Suzumura[‡‡], Keiko Furukawa[‡¶], Yuhsuke Ohmi[‡], Atsushi Natsume[§], Toshihiko Wakabayashi[§], and Koichi Furukawa[‡¶1]

*From the [‡]Department of Biochemistry II, the [§]Department of Neurosurgery, Nagoya University Graduate School of Medicine, 65 Tsurumai, Showa-ku, Nagoya 466-0065, Japan, the [‖]Department of Biochemistry, Faculty of Medicine, Saitama Medical University, 38 Morohongo, Moroyama-machi, Iruma-gun, Saitama 350-0495, Japan, the **Department of Biochemistry, Kochi University Medical School, Kohasu, Okou-cho, Nankoku, Kochi 783-8505, Japan, the [‡‡]Department of Neuroimmunology, Research Institute of Environmental Medicine, Nagoya University, Furou-cho, Chikusa-ku, Nagoya 464-8601, Japan, and the [¶]Department of Biomedical Sciences, Chubu University College of Life and Health Sciences, 1200 Matsumoto-cho, Kasugai 487-8501, Japan*

Background: Roles of GD3 in gliomas are not well understood.
Results: PDGF receptor α was identified as a GD3-associated molecule by enzyme-mediated activation of radical sources and mass spectrometry, and its association with GD3 and Yes leads to increased invasiveness.
Conclusion: GD3 enhances invasiveness by forming a molecular complex.
Significance: GD3/PDGF receptor α·Yes complex is a potential target for glioma therapy.

There have been a few studies on the ganglioside expression in human glioma tissues. However, the role of these gangliosides such as GD3 and GD2 has not been well understood. In this study we employed a genetically engineered mouse model of glioma to clarify the functions of GD3 in gliomas. Forced expression of platelet-derived growth factor B in cultured astrocytes derived from p53-deficient mice resulted in the expression of GD3 and GD2. GD3-positive astrocytes exhibited increased cell growth and invasion activities along with elevated phosphorylation of Akt and Yes kinase. By enzyme-mediated activation of radical sources reaction and mass spectrometry, we identified PDGF receptor α (PDGFRα) as a GD3-associated molecule. GD3-positive astrocytes showed a significant amount of PDGFRα in glycolipid-enriched microdomains/rafts compared with GD3-negative cells. Src kinase family Yes was co-precipitated with PDGFRα, and its pivotal role in the increased cell invasion of GD3-positive astrocytes was demonstrated by silencing with anti-Yes siRNA. Direct association between PDGFRα and GD3 was also shown, suggesting that GD3 forms ternary complex with PDGFRα and Yes. The fact that GD3, PDGFRα, and activated Yes were colocalized in lamellipodia and the edge of tumors in cultured cells and glioma tissues, respectively, suggests that GD3 induced by platelet-derived growth factor B enhances PDGF signals in glycolipid-enriched microdomain/rafts, leading to the promotion of malignant phenotypes such as cell proliferation and invasion in gliomas.

Gangliosides are sialic acid-containing glycosphingolipids that are enriched in glycolipid-enriched microdomain (GEM)[2]/rafts on the plasma membrane of cells (1, 2). Normal adult brain tissues express gangliosides GM1, GD1a, GD1b, and GT1b as major components and express minimal levels of GD3 and GD2 (3, 4). GD3 and GD2 are expressed mainly at early stages of development in the central nervous tissues in mice and other vertebrates. They become almost undetectable in few days postnatal (5). In turn, neuroectoderm-derived tumors such as neuroblastomas and melanomas and T-cell leukemias express ganglioside GD3 and/or GD2 that have been known as cancer-associated antigens (6, 7). Although several reports showed expression of GD3 and GD2 in human gliomas, the roles of these gangliosides have not been demonstrated to date (8, 9).

Glioma is the most common primary brain tumor, and glioblastoma multiforme is the most frequent among gliomas (65%) with a median survival of one year (10, 11). The Cancer Genome Atlas (TCGA) Research Network has established a comprehensive catalogue of genomic abnormalities driving tumorigenesis (12). Among four subsets of GMB, *i.e.* proneural, neural, classical, and mesenchymal, identified by gene expression data from TCGA core samples, amplification of *PDGFRA* and mutation of

* This work was supported by Ministry of Education, Culture, Sports, Science, and Technology of Japan (MEXT) Grants 22117511, 23590371, and 24390078 and Grant-in-aid for Japan Society for the Promotion of Science (JSPS) Postdoctoral Fellows 24.8954.
[1] To whom correspondence should be addressed. Tel.: 81-52-744-2070: Fax: 81-52-744-2069: E-mail: koichi@med.nagoya-u.ac.jp.

[2] The abbreviations used are: GEM, glycolipid-enriched microdomain; GM3, Neu5Acα2,3Galβ1,4Glc-ceramide; GM1, Galβ1,3GalNAc(Neu5Acα2,3)Galβ1,4Glc-ceramide; GD1a, Neu5Acα2,3Galβ1,3GalNAcβ1,4(Neu5Acα2,3)Galβ1,4Glc-ceramide; GD1b, Galβ1,3GalNAcβ1,4(Neu5Acα2,8Neu5Acα2,3)-Galβ1,4Glc-ceramide; GT1b, Neu5Acα2,3Galβ1,3GalNAcβ1,4(Neu5Acα2,8Neu5Acα2,3)Galβ1,4Glc-ceramide; GD3, Neu5Acα2,8Neu5Acα2,3Galβ1,4Glc-ceramide; GD2, GalNAcβ1,4(Neu5Acα2,8Neu5Acα2,3)Galβ1,4Glc-ceramide; EMARS, enzyme-mediated activation of radical sources, PDGF, platelet-derived growth factor; PDGFR, PDGF receptor; RCAS, replication-competent avian leukemia virus splice acceptor; SFK, Src family kinase; FAK, focal adhesion kinase, MTT, 3-(4,5-dimethylthiazol-2-yl)-2,5-diphenyltetrazolium bromide, EdU, 5-ethynyl-2′-deoxyuridine; CAR, chimeric antigen receptor.

TP53 were noted in a subset of proneural glioblastoma multiforme (13).

It is well known that genomic alterations of receptor-tyrosine kinases, including epithelial growth factor receptor and platelet-derived growth factor receptors (PDGFR), are involved in active signal transductions and are hallmarks of gliomas (14). Oncogenic epithelial growth factor receptor expression or high expression of PDGFRα on the cell surface leads to the constitutive activation of RAS/MAPK and PI3K/Akt signal pathways probably involved in the brain tumor evolution (15, 16). Strategies to inhibit binding of ligands to epithelial growth factor receptor or PDGFRα and to block downstream signals have been considered as therapeutic approaches. Because the majority of brain tumors are invasive (17, 18), it is very hard to completely eliminate glioma cells by surgery. Removing normal brain regions together with invading tumor cells might cause disorders in normal brain functions. The elucidation of molecular mechanisms for tumor invasion and the establishment of novel approaches for suppression of invasiveness are urgent challenges of great importance.

Among a number of mouse cancer models produced by genetic engineering (19), the RCAS (replication-competent avian leukemia virus splice acceptor) vector is useful as it allows specific delivery of oncogenes to the astrocyte-linage cells when used for Gtv-a transgenic mice (20). Tv-a, an avian leukemia virus receptor, is expressed under regulation of glial fibrillary acidic protein promoter in Gtv-a mice (21). Indeed, combined expression of mutated KRas and Akt in astrocytes by using the RCAS/Gtv-a system resulted in the induction of gliomas (22). In this study we analyzed the expression and function of GD3 synthase in gliomas by utilizing the RCAS/tv-a system. We demonstrated roles of the products of GD3 synthase, based on the cooperation with PDGFRα and Yes, in the promotion of gliomagenesis and their progression.

Experimental Procedures

Mice—Gtv-a mouse that expresses tv-a under the glial fibrillary acidic protein promoter has been published (21, 23). p53-decifient mice were provided from RIKEN Bioresource Center (Tsukuba, Japan). These mice are mixed genetic backgrounds of C57BL/6, 129, BALB/c, and FVB/N.

Generation of Tumor-bearing Mice—DF-1 (chicken embryonic fibroblast) was maintained in DMEM supplemented with 10% fetal calf serum. To generate virus-producing cells, DF-1 cells were transfected with RCAS retroviral vectors that contain cDNA of HA-tagged PDGFB, HA-tagged $AKT^{MyrD11-60}$, $KRAS^{K12D}$, or β-$catenin^{S37A}$ by using Lipofectamine 2000™ reagent (Life Technologies). Approximately 1×10^4 virus-producing DF-1 cells were injected into right cerebral cortex of newborn p53-deficient Gtv-a mice (postnatal 0.5∼1 day) by using a Hamilton syringe (26 gauge) as described (22). The injection site was determined at the middle point between the temporal edge and longitudinal fissure and at ⅓ from the occipital edge. After 3 weeks of injection of DF-1/RCAS containing cDNA of HA-tagged PDGFB, almost all mice generated brain tumors, and then these tumor-bearing mice were sacrificed. Tumors were diagnosed as glioblastoma by pathological analysis.

Cells and Cell Culture—A murine astrocyte cell line A1 was obtained from JCRB Cell Bank (National Institute of Biomedical Innovation, Osaka, Japan). A1 cells were maintained in DMEM supplemented with 10% FCS at 37 °C in 5% CO_2.

Preparation of Primary Astrocytes—Primary mixed glial cell cultures were prepared from newborn mice and maintained in DMEM supplemented with 10% FCS. To remove contaminated microglia, trypsinized cells were plated on a Petri dish and incubated for 20 min. Because microglia tends to attach on Petri dishes more strongly than astrocytes, astrocytes were enriched by collecting unattached cells (24, 25). After repeating enrichment procedure three times, almost all cells expressed glial fibrillary acidic protein proteins as tested by immunocytochemical analysis.

Antibodies and Regents—Mouse anti-GD3 monoclonal antibody (R24) was obtained from Dr. L. J. Old (Memorial Sloan-Kettering Cancer Center). Cholera toxin B subunit-biotin conjugate reacting with GM1 is from List Biological Labs (Campbell, CA). Antibodies against gangliosides GM2, GD1a, GD2, GD1b, and GT1b were generated in our laboratory (26). Rabbit anti-PDGFRα antibody, rabbit anti-PDGFRβ antibody, mouse anti-Src antibody, rabbit anti-Yes antibody, mouse anti-Fyn antibody, rabbit anti-Lyn antibody, rabbit anti-Flotillin-1 antibody, rabbit anti-phospho-paxillin antibodies (Tyr-31 and Tyr-181), and rabbit anti-phospho-focal adhesion kinase (FAK) antibodies (Tyr-576, Tyr-861, and Tyr-925) were purchased from Santa Cruz Biotechnology (Santa Cruz, CA). Mouse anti-PDGFRβ antibody, rabbit anti-phospho-Akt antibodies (Thr-308 and Ser-473), rabbit anti-phospho-ERK antibody, rabbit anti-ERK antibody, rabbit anti-phospho-Src family kinase (SFK; Tyr-416) antibody, and rabbit anti-phospho-paxillin (Tyr-118) antibody were purchased from Cell Signaling Technology (Beverly, MA). Mouse anti-Yes antibody, mouse anti-paxillin antibody, and mouse anti-FAK antibody were purchased from BD Transduction Laboratories. Mouse anti-β-actin antibody was purchased from Sigma. Rabbit anti-FITC antibody was purchased from Invitrogen. Goat anti-FITC antibody was purchased from Rockland (Gilbertsville, PA). Lipopolysaccharide (LPS) and purified GD2 were purchased form Sigma. Purified GD3 from bovine milk was purchased from Megmilk snow brand (Tokyo, Japan). Bovine brain ganglioside was purchased from Matreya (Pleasant Gap, PA).

Flow Cytometry and Cell Sorting—Cells (3×10^5) were trypsinized and washed with PBS twice. Cells were incubated with primary antibodies in PBS for 1 h on ice. After washing with PBS twice, cells were incubated with a FITC-conjugated anti-mouse IgG antibodies or a FITC-conjugated streptavidin for 45 min on ice. After washing with PBS twice, relative expression levels of gangliosides were analyzed by FACS Calibur™ (BD Biosciences). For sorting GD3-expressing cells, 1×10^7 cells were stained with an anti-GD3 antibody (R24), and positive cells were isolated by FACS Aria II™ (BD Biosciences) according to the manufacturer's protocol. We checked GD3 expression by flow cytometer before each experiment, whereas the expression level of GD3 in the GD3-positive population was well maintained. When reduced GD3 expression was observed, GD3-positive cells stocked just after sorting were thawed and used.

Enzyme-mediated Activation of Radical Sources (EMARS) and Mass Spectrometry Analysis—EMARS reactions and MS analysis were performed as described previously (27). Briefly, G(−) and G(+) cells (5×10^5) were treated with 5 μg/ml of HRP-conjugated monovalent anti-GD3 antibody (R24) in PBS at room temperature for 20 min. After washing with PBS, cells were incubated with fluorescein (FITC)-LC-ASA (FA) solution diluted in PBS (0.1 mM FA/PBS) at room temperature for 15 min with light shielding. After washing twice with PBS, the treated cells were scraped with 100 mM Tris-HCl, pH 7.4, and 1 mM phenylmethylsulfonyl fluoride (PMSF). The labeled molecules with FITC were immunoprecipitated with anti-FITC antibody (Invitrogen) and served for MS analysis. HRP-conjugated monovalent anti-GD3 antibody (R24) was prepared by using peroxidase labeling kit-SH™ (DOJINDO, Kumamoto, Japan). Immunoprecipitates were dissolved in MS sample buffer (12 mM sodium deoxycholate, 12 mM sodium lauroylsarcosine, 100 mM Tris-HCl, pH 8.0), boiled at 95 °C, and centrifuged at 20,000 × *g* for 10 min. The supernatants underwent reduction with dithiothreitol and alkylation with iodoacetamide. Then the samples were 5-fold diluted with 50 mM ammonium bicarbonate and digested by Lys-C (Wako, Osaka, Japan) for 3 h and then by trypsin (Promega, Madison, WI) for 8 h at 37 °C. They were desalted and concentrated with C18 StageTips™. MS was performed using an LTQ-Orbitrap-XL™ mass spectrometer (Thermo-Fisher Scientific, Waltham, MA) system combined with a Paradigm MS4 HPTLC System™ (Michrom BioResources Inc., Auburn, CA). MS/MS spectra was submitted to the program Mascot 2.3™ (Matrix Science, Boston, MA) and X! Tandem™ (The GPM) for MS/MS ion search. Mascot was set up to search the Sprot_2013_6 database (selected for *Mus musculus*, 16,671 entries) assuming the digestion enzyme trypsin.

Western Blotting—After washing with PBS three times, cells were lysed by cell lysis buffer (20 mM Tris-HCl, pH 7.5, 150 mM NaCl, 1 mM Na_2EDTA, 1 mM EGTA, 1% Triton X-100, 2.5 mM sodium pyrophosphate, 1 mM β-glycerophosphate, 1 mM Na_3VO_4, and 1 μg/ml leupeptin) (Cell Signaling Technology) supplemented with protease inhibitor mixture (Merck). Cell lysates were sonicated briefly and centrifuged at 14,000 × *g* for 10 min to remove insoluble materials. Proteins in supernatants were measured by DC™ protein assay (Bio-Rad), and 20 μg of total proteins were separated in SDS-PAGE using 10% gels. Separated proteins were transferred onto an Immobilon-P™ membrane (EMD Millipore, Billerica, MA), and blots were incubated with 5% skim milk in PBS including 0.05% Tween 20 for blocking. The membrane was probed with primary antibodies and HRP-labeled secondary antibodies sequentially, and bound conjugates on the membrane were visualized with an Enhanced Chemiluminescence™ detection system (PerkinElmer Life Sciences).

Thin Layer Chromatography (TLC); Immunostaining—Total lipids in raft fractions or immunoprecipitates were extracted by treating with chloroform/methanol mixture (2:1, v/v). After drying the solvents under N_2 gas stream, lipids were dissolved in distillated water and loaded to Sep-Pak (Waters, Milford, MA). After washing with distillated water, lipids were eluted by methanol, chloroform/methanol mixture (2:1 and 1:1, v/v) sequentially. The extracts were dried under N_2 gas stream and dissolved in 30 μl of chloroform/methanol (2:1, v/v). The total volume of extracted lipids was separated using high performance TLC plates (Merck). These lipids were developed using a solvent system of chloroform, methanol, 0.22% $CaCl_2$ (55:45:10, v/v/v) and blotted onto a polyvinylidene difluoride membrane (Atto, Tokyo, Japan) using TLC Thermal Blotter, AC-5970 (Atto). After blocking with 3% BSA in PBS, the membrane was probed with an anti-GD3 monoclonal antibody (mAb), an anti-GD2 mAb, an anti-GD1b mAb, or an-anti-GT1b mAb and sequentially with an HRP-labeled anti-mouse IgG or anti-mouse IgM antibody. Bound conjugates on the membrane were visualized with an Enhanced Chemiluminescence™ detection system (PerkinElmer Life Sciences).

TABLE 1
Primers in this study

Genes	Forward	Reverse
St8sia1	AAAGGACGGGATGGGGGATA	CCGCTTGCAAATCCACAACA
PDGFRα	CAGGTCTTTGTGCAACCAGC	CCAAAGCGTCACCTGCTAGA
PDGFRβ	CCTCAAAAGTAGGTGTCCACGA	GGTGACCTCCTGCGAATCTC
Gapdh	GGTGCTGAGTATGTCGTGGA	CCTTCCACAATGCCAAAGTT
Lcn2	GGACTACAACCAGTTCGCCA	CCACACTCACCACCCATTCA
Ifi202b	ACCGGTGTCATTTTCTTACCA	AGGGGTCTGATGTTGACCCT
Clcf1	TGTTACTTGCGTGGCCTCAA	CAGCAGCCAGAAGTCATCCA
Steap4	ACCTCCCTGGTATTCTCGCT	AGGGCCTGAGTAATGGTTGC
H2-t23	ACACTCGCTGCGGTATTTCA	AGCGTGTGAGATTCGTCGTT
Timp1	CCCCAGAAATCAACGAGACCA	GTACGCCAGGGAACCAAGAA

Immunoprecipitation—Cells were lysed with MNE buffer (25 mM MES, pH 6.5, 150 mM NaCl, 5 mM EDTA, 1 mM Na_3VO_4, 1 mM PMSF, 1 μg/ml aprotinin) containing 1% Triton X-100. Lysates were centrifuged at 14,000 × *g* for 10 min at 4 °C to remove insoluble materials and immunoprecipitated with primary antibodies at 4 °C overnight with rotation. Then protein G-Sepharose or A-Sepharose (GE Healthcare) was added and rotated at 4 °C for 2 h. The beads were washed 3 times with MNE buffer containing 0.5% Triton X-100, and the precipitated proteins were separated with SDS-PAGE to be used for immunoblotting.

Quantitative Polymerase Chain Reaction—Extraction of RNAs was performed by using TRIzol™ reagent (Ambion, Life Technologies) following the manufacturer's protocol. cDNA was generated using oligo(dT) primer and Moloney murine leukemia virus reverse transcriptase (Invitrogen). The quantitative PCR was carried out using DyNAmo SYBR Green™ qPCR kit (Thermo Fisher Scientific, Waltham, MA) and CFX Connect™ Real-Time System (Bio-Rad). Primers used in this study are listed in Table 1.

Sucrose Density Gradient Fractionation of Triton X-100 Extracts—Cells ($1–2 \times 10^7$) were lysed by MNE buffer containing 1% Triton X-100. After removing insoluble materials by centrifugation at 14,000 × *g* for 10 min, lysates were Dounce-homogenized 10 times with Digital Homogenizer™ (As One, Osaka, Japan). The lysates were mixed with an equal volume of 80% sucrose in MNE buffer, and a stepwise gradient was prepared by overlaying 30% sucrose in MNE buffer followed by a final layer of 5% sucrose in MNE buffer. The gradient was formed by centrifugation for 14–16 h at 4 °C at 100,000 × g using a MLS50 rotor (Beckman Coulter Inc., Brea, CA). Fractions of 500 μl were separated from the top of the gradient and used for Western blotting.

Immunocytochemistry—Cells (2×10^5) were plated on a glass-bottom dish (Iwaki, Tokyo, Japan) precoated with 0.01%

poly-L-lysine (Sigma) and incubated for 24 h in DMEM supplemented with 10% FCS. After washing 3 times with PBS, cells were fixed with 4% paraformaldehyde in PBS for 10 min at room temperature. Then dishes were blocked with 2.5% BSA in PBS for 1 h and incubated with an anti-GD3 mAb, an anti-PDGFRα antibody, or an anti-Yes antibody diluted in 0.5% BSA in PBS. After incubation with primary antibodies for 1 h at room temperature, dishes were washed with PBS and incubated with an Alexa 568-conjugated anti-mouse IgG antibody (Invitrogen) and an Alexa 488-conjugated anti-rabbit IgG antibody (Invitrogen) in 0.5% BSA in PBS for 1 h at room temperature. After washing the dishes with PBS, DAPI staining was performed, and cells were observed under a confocal microscopy (Fluoview FV10i, Olympus, Tokyo, Japan). For staining with an-anti Yes antibody, cells were serum-starved for 16 h and incubated with DMEM supplemented with 10% FCS for 30 min before fixation. In addition, a permeabilization procedure was performed by incubation with 0.1% Triton X-100 in PBS before blocking.

Immunohistochemistry—Brain tissues were fixed with 4% paraformaldehyde in PBS overnight at 4 °C. Then the solution was replaced sequentially with 10% sucrose, 15% sucrose, and 20% sucrose and embedded in optimum cutting temperature (O.C.T.™) compound (Sakura Finetechnical, Tokyo, Japan) and frozen in liquid nitrogen. Ten-micrometer-thick frozen sections were prepared with a cryostat (CM3050S, Leica, Wetzlar, Germany). After drying, sections were blocked with 1% BSA in PBS containing 0.075% Tween 20 at room temperature for 1 h and stained with primary antibodies and suitable secondary antibodies sequentially. Antibodies were diluted in 1% BSA in PBS containing 0.01% Tween 20. After incubation with secondary antibodies, sections were washed with PBS 3 times and mounted on 90% glycerol. Sections were observed under a confocal microscope (Fluoview FV10i™, Olympus).

3-(4,5-D+imethylthiazol-2-yl)-2,5-diphenyl-tetrazolium Bromide (MTT) Assay—Cells (1×10^3) were plated on 96-well plates with DMEM supplemented with 10% FCS. After culturing for 0.5, 1, 2, or 3 days, 20 μl of a 5 mg/ml MTT solution in PBS was added and incubated for 4 h at 37 °C. The reaction was stopped by adding 1-propanol containing 0.4% HCl and 0.1% Nonidet P-40. The absorption values at 590 nm were then determined using an automatic plate reader (ImmunoMini NJ-2300, Nalgene Nunc, NY).

Migration and Invasion Assay—Invasion assay was performed with cell culture inserts (Transparent PET™ Membrane, 24-well, 8.0-μm pore size; BD Falcon). Matrigel™ (BD Bioscience) was diluted in ice-cold PBS (200 μg/ml), and the solution (200 μl) was added to the upper chamber. After being left to be polymerized for 2 h at room temperature, the membrane was reconstituted with serum-free DMEM for 1 h, and the lower chamber was filled with DMEM supplemented with 10% FCS. After removing medium, cells (2×10^4) in serum-free DMEM were added in the upper chamber and incubated for 24 h. After incubation, cells on the surface of the membrane were stained with Giemsa (Wako), and cell number was counted under a microscopy (CKX41™, Olympus). In a migration assay, the same procedure was performed without Matrigel.

Uptake of 5-Ethynyl-2′-deoxyuridine (EdU)—Measurement of cell proliferation was carried out using Click-It EdU™ Imaging kits (Invitrogen). After transfection of siRNAs, cells were cultured in DMEM supplemented with 10% FCS for 24 h, and then the medium was changed to DMEM supplemented with 0.1% FCS and 10 μM EdU. After further incubation for 24 h, cells were fixed and incorporated EdU was stained following the manufacturer's protocol. EdU-positive cells were counted under the fluorescence microscopy (BX51, Olympus).

Knockdown of Yes in Primary Astrocytes—Yes-specific siRNA or scramble siRNA (4 μg) were transfected into 1×10^6 cells by electroporation using Amax a Basic Nucleofector™ kit for Primary Mammalian Glial Cells (Lonza, Gampel Valais, Switzerland). The sequences of three kinds of siRNA for Yes were 5′-GGAUUAUGCCACAAGUUAATT-3′ (#1), 5′-GGUUAUAUCCCUAGCAAUUTT-3′ (#2), and 5′-GUUAUAUCCCUAGCAAUUATT-3′ (#3). These siRNAs were purchased from Sigma.

Statistics—Mean values were compared using an unpaired Student's two-tailed *t* test. *p* values of < 0.05 were considered statistically significant.

Study Approval—All experimental protocols using mice were approved by the animal experimental committee of the Graduate School of Medicine in Nagoya University along the guidelines of Japanese government.

Results

Transfection of PDGFB Resulted in the Expression of GD3 in Primary Astrocytes—At first, we prepared primary cultures of astrocytes from newborn Gtv-a mice and transfected various cDNAs of oncogenic genes such as *PDGFB*, *AKT*, *KRAS*, or β-catenin by using RCAS vector. Primary cultured astrocytes from Gtv-a mice expressed tv-a, a receptor for RCAS. After infection of various RCAS vectors, we analyzed relative expression levels of GD3 and GD2 on astrocytes by flow cytometry. Analysis of ganglioside expression on astrocytes from p53 wild type Gtv-a mice revealed that transfection of any of these cDNAs did not bring about expression of GD3 or GD2 (Fig. 1, *upper two rows*). On the other hand, when astrocytes from p53-decifient Gtv-a mice were analyzed, GD3 expression was found in a small population of astrocytes transfected with PDGFB cDNA (Fig. 1, *lower two rows*). These data suggested that GD3 expression was induced in astrocytes by PDGFB under p53-deficient conditions.

GD3-positive Astrocytes Showed Aggressive Phenotypes—To investigate whether induced GD3 leads to malignant phenotypes in astrocytes, cell growth, migration, and invasion activities in GD3-expressing (G(+)) cells and GD3-negative (G(−)) cells were tested. After staining PDGFB-transfected p53-deficient primary cultured astrocytes with an anti-GD3 mAb, they were sorted into G(+) population (*P2* region in Fig. 2*A*) and G(−) population (*P1* region in Fig. 2*A*). After sorting three times, we established two lines, G(+) and G(−),as shown in Fig. 2*B*. In fact, forced expression of PDGFB resulted in the change in expression profiles of gangliosides in astrocytes. Although non-transfected primary cultured astrocytes and G(−) cells expressed GM1 alone, G(+) cells expressed GM1, GD3, GD2, GD1b, and GT1b (Fig. 2, *C–E*). Using these cells, we examined mRNA expression levels of St8sia1 (GD3 synthase) by quantitative RT-PCR. Corresponding with GD3 expression, G(+)

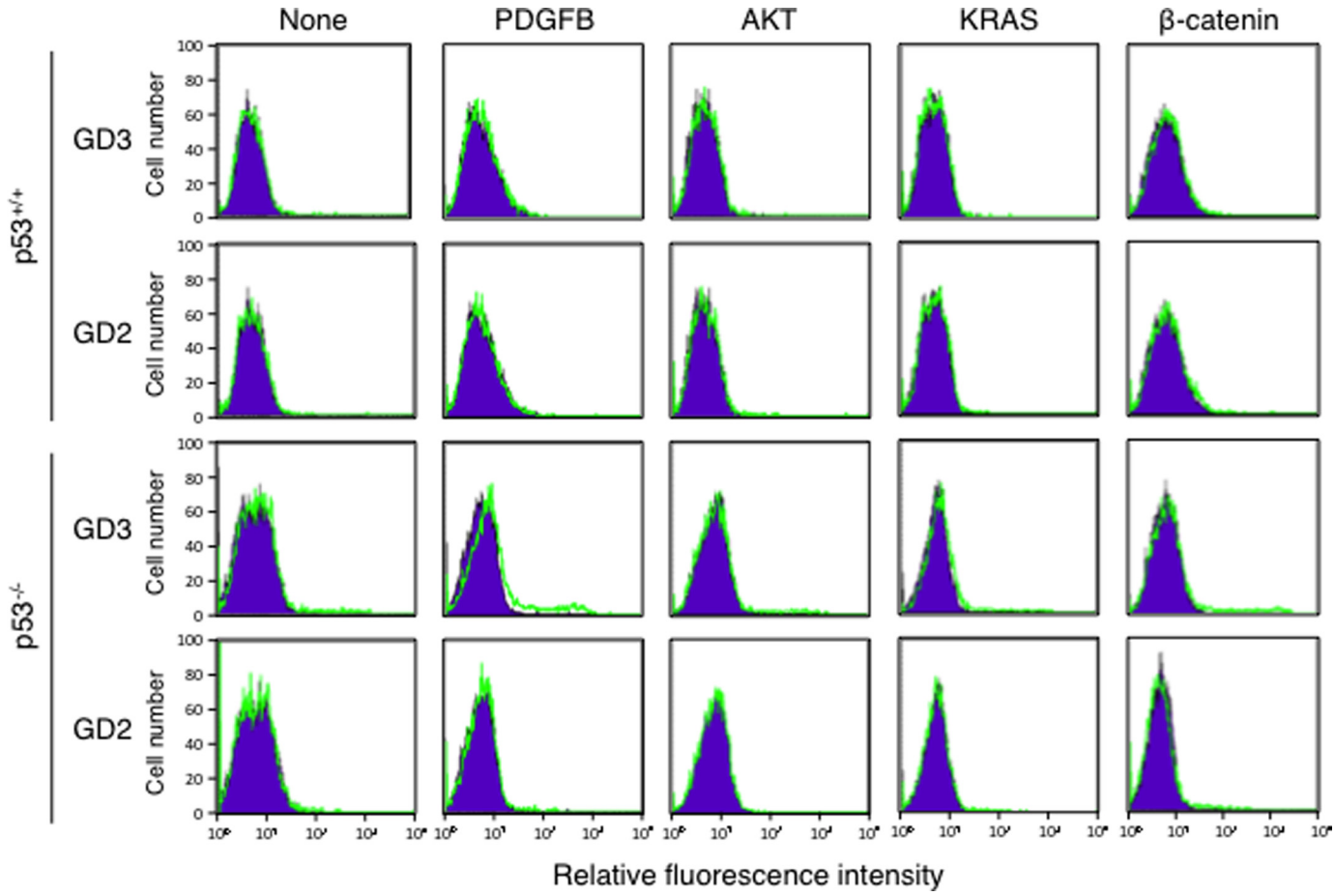

FIGURE 1. **PDGFB transfection resulted in the induction of GD3 in p53$^{-/-}$ astrocytes.** After transfection of *PDGFB*, *AKT*, *KRAS*, or β-catenin in RCAS vector or vector alone into primary cultured astrocytes prepared from newborn mice, cells (3×10^5) were detached by treatment with trypsin. After washing, cells were incubated with an anti-GD3 mAb or an anti-GD2 mAb for 1 h on ice. After washing, they were incubated with an FITC-labeled anti-mouse IgG antibody. Expression levels of GD3 and GD2 were analyzed by flow cytometry. The results of astrocytes from wild type Gtv-a mice were shown in the *upper two panels*, and those of astrocytes from p53$^{-/-}$ Gtv-a mice were shown in the *lower two panels*. *Green lines* indicate the cells stained with either one of mAbs. *Blue lines* indicate the cells stained with a non-relevant antibody for control.

cells expressed higher levels of St8sia1 gene than G(−) cells (Fig. 3*A*). It has been known that GD3 expression is observed in reactive astrocytes (28–30). Gene expression analysis of reactive astrogliosis induced by transient ischemia or injection of LPS showed significant up-regulation of genes such as *Lcn2*, *Ifi202b*, *Clcf1*, *Steap4*, *H2-T23*, or *Timp1* (31). Then we examined mRNA expression levels of *Lcn2*, *Ifi202b*, *Clcf1*, *Steap4*, *H2-T23*, and *Timp1* gene in G(−) and G(+) cells to clarify whether G(+) cells could be characterized as reactive astrocytes. As shown in Fig. 3*A*, G(+) cells showed lower expression of *Clcf1* and *Timp1* genes than G(−) cells, and G(+) cells did not express *Lcn2*, *Ifi202b*, and *H2-T23* genes. Therefore, G(+) cells were not necessarily characterized as reactive astrocytes despite GD3 expression. Then we analyzed the cell growth rate of GD3(−) and GD3(+) cells by using the MTT assay. As shown in Fig. 3*B*, G(+) cells showed higher cell growth rates than G(−) cells. Furthermore, G(+) cells showed significantly higher migration and invasion activity than G(−) cells (Fig. 3*C*). These data indicate that expression of GD3 by PDGFB enhances malignant phenotypes in astrocytes.

Yes Was Phosphorylated in GD3-positive Astrocytes—Phosphorylation levels of Akt, ERKs, and SFKs such as Src, Yes, Lyn, and Fyn in G(+) and G(−) cells, were examined by Western blotting. G(+) cells showed higher phosphorylation levels of Akt and some SFKs than G(−) cells, whereas no differences in phosphorylation levels of ERKs between G(+) and G(−) cells were detected (Fig. 3*D*). Both G(+) and G(−) cells expressed no Fyn or Lyn. Although anti-p-SFKs (Tyr-416) antibody reacts with phosphorylated forms of almost all SFKs including Src and Yes, immunoprecipitation-immunoblotting experiments revealed that Yes, but not Src, was phosphorylated more intensely in G(+) than in G(−) cells (Fig. 3*E*).

PDGFRα Is Associated with GD3 in Astrocytes—Gangliosides are expressed mainly on plasma membranes and are localized in GEM/rafts. It is known that gangliosides play as a fine tuner of cell signaling by modulating the molecular composition in GEM/rafts (32). Tumor-specific ganglioside GD3 could modulate functions of plasma membrane proteins by interacting with them, leading to enhanced malignant phenotypes. To address this issue we tried to identify GD3-associated molecules by EMARS using G(+) and G(−) cells. In this system molecules located within 200–300 nm in diameter of GD3 can be labeled with FITC by radical reaction of an aryl azide functional group (33). FITC-labeled molecules were collected by immunoprecipitation using an anti-FITC antibody as shown in Fig. 4*A*. Using these immunoprecipitates, we performed LC-MS/MS analysis to iden-

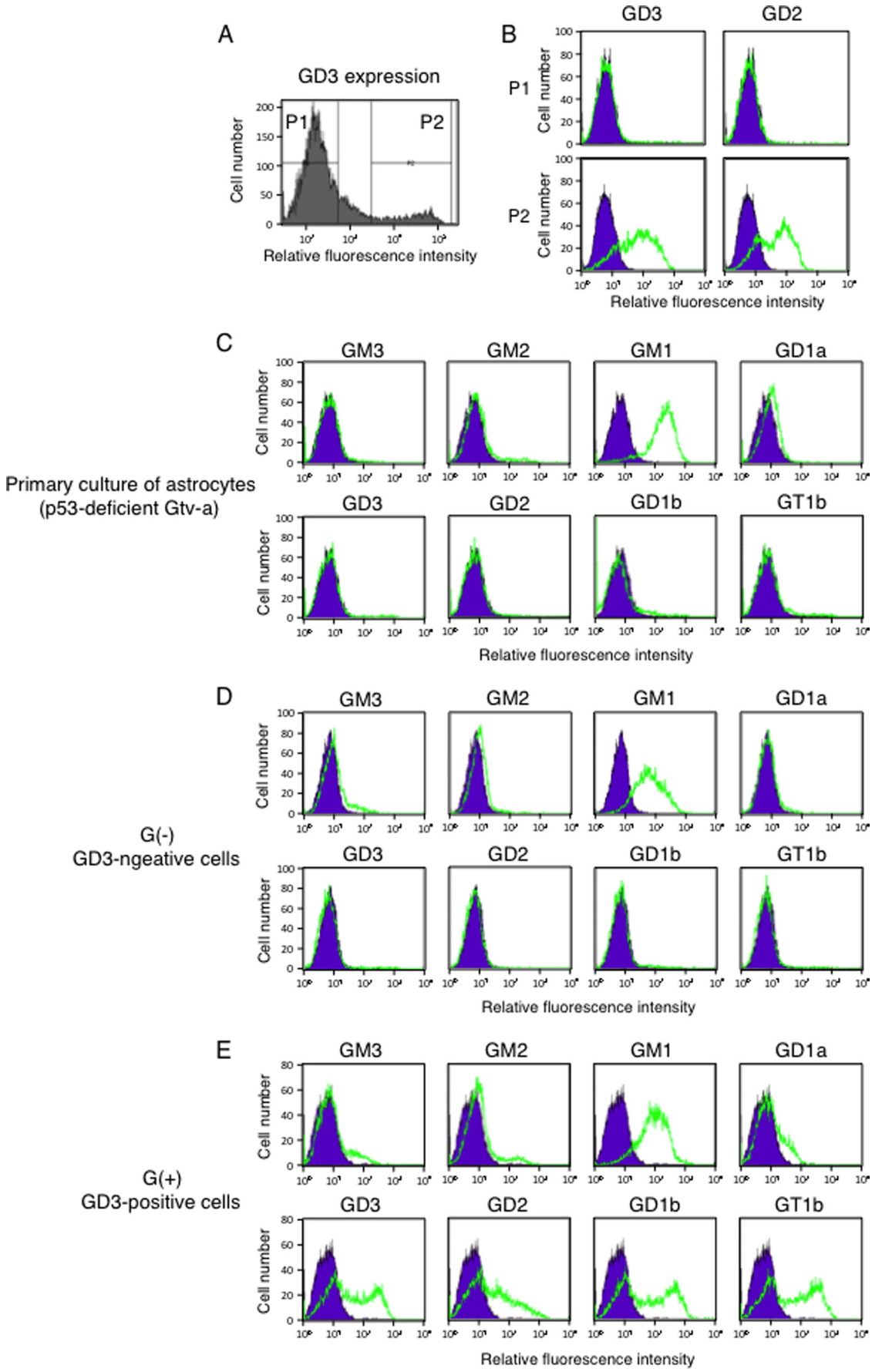
A
GD3 expression
P1
P2
Cell number
Relative fluorescence intensity
B
GD3
GD2
P1
P2
Cell number
Relative fluorescence intensity
C
Primary culture of astrocytes
(p53-deficient Gtv-a)
GM3
GM2
GM1
GD1a
GD3
GD2
GD1b
GT1b
Cell number
Relative fluorescence intensity
D
G(-)
GD3-ngeative cells
GM3
GM2
GM1
GD1a
GD3
GD2
GD1b
GT1b
Cell number
Relative fluorescence intensity
E
G(+)
GD3-positive cells
GM3
GM2
GM1
GD1a
GD3
GD2
GD1b
GT1b
Cell number
Relative fluorescence intensity

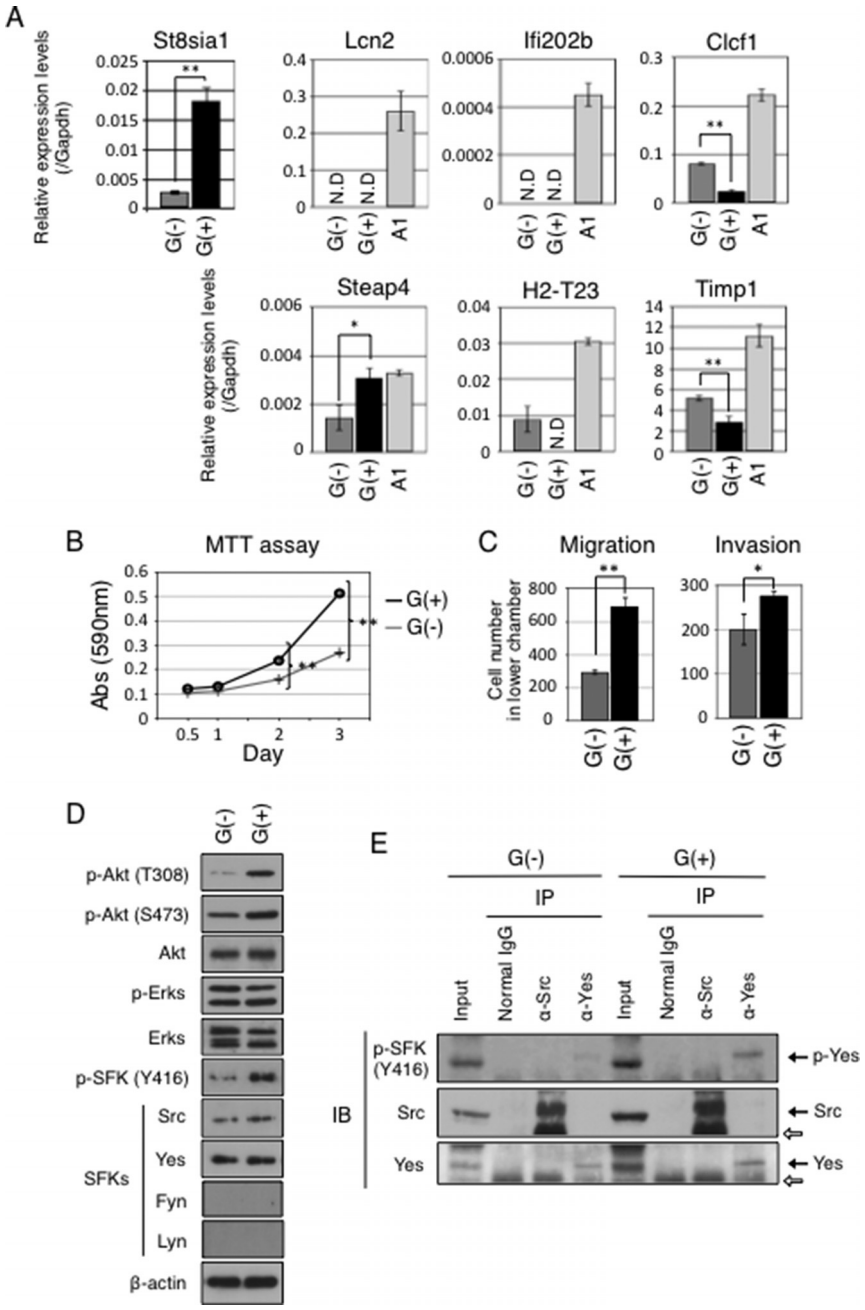

FIGURE 3. **GD3-positive cells showed distinct gene expression patterns from those of reactive astrocytes and enhanced malignant properties with increased phosphorylation levels of Akt and Yes kinases compared with GD3-negative cells.** *A*, mRNA expression levels of St8sia1, Lcn2, Ifi202b, Clcf1, Steap4, H2-T23, and Timp1 in G(−) and G(+) cells were examined by quantitative RT-PCR. Expression levels were normalized with Gapdh data. mRNA expressions in LPS-stimulated A1 cells (100 ng/ml) were also analyzed. *N.D.*, not detected. *, $p < 0.05$; **, $p < 0.01$. *B*, cell growth in G(+) and G(−) cells measured by MTT assay. Cells (1×10^3) were plated in 96-well plates in DMEM supplemented with 10% FCS at day 0, then cell growth was measured at days 0.5, 1, 2, and 3. The *black line* indicates G(+) cells, and the *gray line* indicates G(−) cells. **, $p < 0.01$. *C*, migration and invasion activities in G(+) and G(−) cells measured using cell culture inserts. Two $\times 10^4$ cells were plated in the upper chamber in serum-free medium. The lower chamber contained DMEM supplemented with 10% FCS. After incubation for 24 h, invaded cells to the reverse side of membrane were counted after Giemsa staining. When invasion activities were measured, chambers were pre-coated with Matrigel™ (50 μg) as described under "Experimental Procedures." *Black bars* indicate G(+) cells, and *gray bars* indicate G(−) cells. *, $p < 0.05$; **, $p < 0.01$. *D*, phosphorylation levels of Akt, ERKs, and SFKs in G(+) cells and G(−) cells were examined by Western blotting. Used antibodies were indicated at the *left side of the bands*. *E*, results of immunoprecipitation (*IP*)-immunoblotting (*IB*) experiments. Immunoprecipitates prepared from the lysates of G(−) and G(+) cells (4×10^5) with an anti-Src or an anti-Yes antibody were analyzed by Western blotting. The *white arrows* indicate IgG heavy chains.

FIGURE 2. **Establishment of GD3-positive cells and GD3-negative cells.** *A*, expression levels of GD3 in PDGFB-transfected $p53^{-/-}$ astrocytes were analyzed by flow cytometry. Cells in P1 and P2 regions were sorted as GD3-positive (G(+)) and GD3-negative (G(−)) cells. *B*, expression levels of GD3 and GD2 in P1 and P2 regions of PDGFB-transfected $p53^{-/-}$ astrocytes after sorting were examined by flow cytometry. *C–E*, expression profiles of gangliosides in astrocytes. Expression levels of GM3, GM2, GM1, GD1a, GD3, GD2, GD1b, and GT1b in primary cultured astrocytes prepared from $p53^{-/-}$ Gtv-a mice (non-transfectant cells) (*C*), G(−) cells (*D*), and G(+) cells (*E*) were analyzed by flow cytometry as described in Fig. 1. Cells (3×10^5) were incubated with each anti-ganglioside antibody for 1 h on ice, then cells were washed with PBS and incubated with an FITC-labeled anti-mouse IgG antibody for 45 min on ice. Relative expression levels of gangliosides were examined by FACS Calibur™. *Green lines* indicate the cells stained with individual anti-ganglioside antibodies. *Blue lines* indicate the cells stained with non-relevant antibodies as controls.

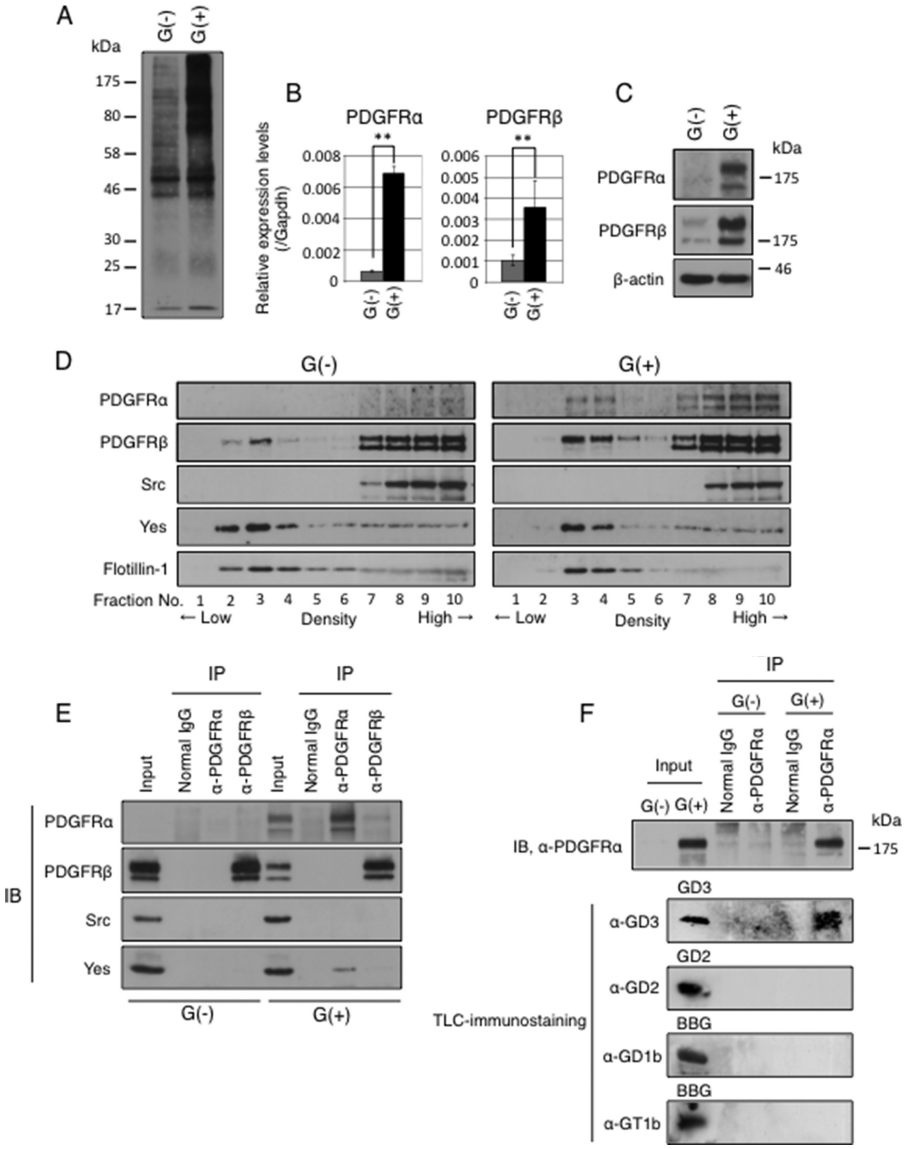

FIGURE 4. **PDGFRα was identified as a GD3-associated molecule in astrocytes.** *A*, labeling pattern with EMARS reaction. Cell lysates from G(+) and G(−) cells after EMARS reaction were applied for immunoprecipitation using a rabbit anti-FITC antibody. The immunoprecipitates were separated by SDS-PAGE and subsequently immunoblotted using goat anti-FITC antibodies. *B*, expression levels of PDGFRα and PDGFRβ mRNA measured by quantitative RT-PCR. Expression levels were normalized with Gapdh data. **, $p < 0.01$. *C*, expression levels of PDGFRα and PDGFRβ proteins in G(+) and G(−) cells were analyzed by Western blotting. *D*, floating patterns of PDGFRα, PDGFRβ, Src, and Yes in G(+) and G(−) cells were examined by Western blotting. Sucrose density gradient fractionations of 1% Triton X-100 extracts were performed. Low-number fractions indicate low density fractions. Flotillin-1 was used as a GEM/raft maker. *E*, results of immunoprecipitation (*IP*)-immunoblotting (*IB*) experiments. After serum starvation for 14 h, cells (4×10^5) were cultured in DMEM containing 10% FCS for 30 min. Then cells were lysed, and immunoprecipitation was performed with an anti-PDGFRα or an anti-PDGFRβ antibody. PDGFRα, PDGFRβ, Yes, and Src in immunoprecipitates were detected by Western blotting. *F*, Cells (1×10^7) were lysed by 1% saponin in MNE buffer, and the lysates were served for immunoprecipitate-TLC-immunostaining experiments. Immunoprecipitates prepared by an anti-PDGFRα antibody were served for Western blotting with an anti-PDGFRα antibody (*upper panel*) or for TLC-immunostaining with an anti-GD3 mAb, an anti-GD2 mAb, an anti-GD1b mAb, or an-anti-GT1b mAb (*lower panels*). In TLC immunostaining, purified GD3 (0.5 μg), GD2 (0.5 μg), and bovine brain gangliosides (*BBG*, 5 μg) were used as standards at the *left end*.

tify the labeled molecules and succeeded in identifying 37 plasma membrane proteins as GD3-associated molecules in G(+) cells (Table 2). Among them, PDGFRα was identified as one of the GD3-associated molecules. In quantitative reverse transcription-PCR and Western blotting, G(+) cells expressed higher levels of PDGFRα than G(−) cells (Fig. 4, *B* and *C*).

Both Yes and GD3 Were Co-precipitated with PDGFRα in GD3-positive Astrocytes—To analyze floating patterns of PDGFRα, PDGFRβ, Src, and Yes, Western blotting as performed using fractions prepared by sucrose density -gradient ultracentrifugation of 1% Triton X-100 extracts from G(+) and G(−) cells. As shown in Fig. 4*D*, a part of PDGFRα was definitely localized in GEM/rafts in G(+) cells: the majority of Yes, but not Src, was also localized in GEM/rafts fraction both in G(+) and G(−) cells. Binding of Yes to PDGFRα in G(+) cells would be expected. In fact, Yes was co-precipitated with an anti-PDGFRα antibody but not by an anti-PDGFRβ antibody in G(+) cells as shown in Fig. 4*E*.

Then we examined whether PDGFRα binds to GD3 in astrocytes by immunoprecipitate-TLC immunostaining. Using

TABLE 2
Identified plasma membrane proteins as candidates of GD3-associated proteins in astrocytes by EMARS/MS

No.	Protein name	Accession
1	Usherin	USH2A_MOUSE
2	FRAS1-related extracellular matrix protein 2	FREM2_MOUSE
3	Probable G-protein-coupled receptor 112	GP112_MOUSE
4	Down syndrome cell adhesion molecule homolog	DSCAM_MOUSE
5	Sialoadhesin	SN_MOUSE
6	Receptor-type tyrosine-protein phosphatase C	PTPRC_MOUSE
7	Phosphorylase *b* kinase regulatory subunit α, liver isoform	KPB2_MOUSE
8	Protein jagged-1	JAG1_MOUSE
9	Angiopoietin-1 receptor	TIE2_MOUSE
10	SH3 and PX domain-containing protein 2A	SPD2A_MOUSE
11	Platelet-derived growth factor receptor α	PGFRA_MOUSE
12	Guanine nucleotide-binding protein G subunit α isoforms XLas	GNAS1_MOUSE
13	Microtubule-associated protein 4	MAP4_MOUSE
14	Leucyl-cystinyl aminopeptidase	LCAP_MOUSE
15	Ephrin type-A receptor 2	EPHA2_MOUSE
16	Potassium voltage-gated channel subfamily KQT member 3	KCNQ3_MOUSE
17	Calpain-3	CAN3_MOUSE
18	Disintegrin and metalloproteinase domain-containing protein 9	ADAM9_MOUSE
19	Plastin-2	PLSL_MOUSE
20	Baculoviral IAP repeat-containing protein 2	BIRC2_MOUSE
21	MAGUK p55 subfamily member 6	MPP6_MOUSE
22	Bardet-Biedl syndrome 4 protein homolog	BBS4_MOUSE
23	TNF receptor-associated factor 4	TRAF4_MOUSE
24	Thymic stromal cotransporter protein	TSCOT_MOUSE
25	Ras GTPase-activating protein-binding protein 1	G3BP1_MOUSE
26	Tubulin β-5 chain	TBB5_MOUSE
27	Ankyrin repeat and SAM domain-containing protein 4B	ANS4B_MOUSE
28	LanC-like protein 1	LANC1_MOUSE
29	Annexin A2	ANXA2_MOUSE
30	3-Keto-steroid reductase	DHB7_MOUSE
31	Guanin nucleotide-binding protein G subunit β-2	GBB2_MOUSE
32	Vesicle-associated membrane protein-associated protein A	VAPA_MOUSE
33	Tumor necrosis factor receptor superfamily member 9	TNR9_MOUSE
34	Ras-related protein Ral-B	RALB_MOUSE
35	Cell division control protein 42 homolog	CDC42_MOUSE
36	Ras-related C3 botulinum toxin substrate	RAC1_MOUSE
37	Ubiquitin-conjugating enzyme E2 D3	UB2D3_MOUSE

immunoprecipitates from G(+) cells and G(−) cells with an anti-PDGFRα antibody, TLC-immunostaining was performed with an anti-GD3 antibody, an anti-GD2 antibody, an anti-GD1b antibody, or an anti-GT1b antibody. Consequently, GD3 was detected, but GD2, GD1b, or GT1b was not detected in the immunoprecipitates (Fig. 4*F*). These results suggested that a molecular complex consisting of GD3, PDGFRα, and Yes was formed in GEM/rafts in G(+) cells. PDGFRα is recruited to GEM/rafts by binding to GD3, which then might facilitate binding with Yes. This complex of GD3/PDGFRα/Yes could induce activation of Yes, leading to enhanced signals for malignant phenotypes. Immunocytochemistry revealed that PDGFRα and GD3 were co-localized at the leading edge of G(+) cells (Fig. 5, *A* and *B*). Moreover, Yes was also co-localized with PDGFRα in G(+) cells (Fig. 5, *C* and *D*).

Yes Is Involved in the Invasion Activity in Astrocytes—To clarify roles of Yes, knockdown of Yes in astrocytes was performed using siRNA. At first, we prepared three kinds of anti-Yes siRNA (#1, #2, and #3) and tested knockdown efficiency of Yes in G(+) cells. Transfection of anti-Yes siRNA (#2) suppressed Yes expression with the highest efficiency (Fig. 6*A*). After knockdown of Yes using anti-Yes siRNA (#2), cell growth rates were tested by measuring incorporation of EdU. As shown in Fig. 6*B*, counts of EdU-positive cells showed no significant differences between anti-Yes siRNA-transfected cells and scramble siRNA-transfected cells. These results indicated that Yes is scarcely involved in cell growth in both G(+) and G(−) cells. Invasion assays were performed using the Yes-silenced cells. Interestingly, the number of invasive cells was dramatically reduced in both G(+) and G(−) cells after knockdown of Yes (Fig. 6*C*). Although there were no significant differences in the phosphorylation levels of Akt, ERKs, and FAK between anti-Yes siRNA-transfected cells and scramble siRNA-transfected cells, phosphorylation levels of paxillin were definitely suppressed after knockdown of Yes in both G(+) cells and G(−) cells (Fig. 6, *D* and *E*). It is well known that the phosphorylation of paxillin is required for cell adhesion and invasion (34). Therefore, these data suggested that Yes is involved in the invasion activities via the activation of paxillin, a key protein as a downstream target of Yes in G(+) astrocytes. We also examined phosphorylation levels of paxillin after knockdown of Yes by using anti-Yes siRNA (#3) in G(+) and G(−) cells. Phosphorylation levels of paxillin were decreased as in cells treated by anti-Yes siRNA (#2) (Fig. 6*E*, *right panels*).

Expression of GD3, PDGFRα, and Yes in Gliomas—Finally, we analyzed primary culture of glioma cells derived from PDGFB-transfected brain tissues in p53-decificent Gtv-a mice. Because gliomas were generated by injection of RCAS/PDGFB into cortex of right brain of p53-decificent Gtv-a mouse, we prepared a primary culture of glioma cells from the glioma region in the right brain. We also prepared primary culture cells from the opposite side of virus-injected brain in the same mouse as a control. In accordance with the results using primary cultured astrocytes, primary cultured glioma cells also expressed GD3, GD2, and PDGFRα more strongly as compared with primary cultured control cells (Fig. 7, *A*–*C*).

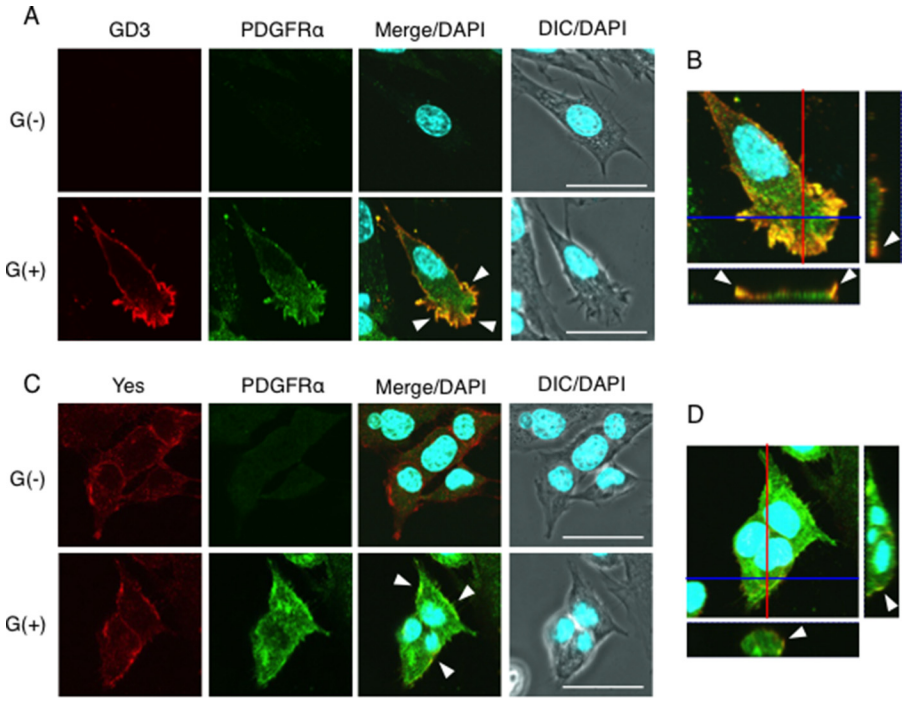

FIGURE 5. **PDGFRα was co-localized with GD3 and Yes kinase in GD3-positive astrocytes.** *A*, immunocytochemical staining of G(−) cells and G(+) cells with an anti-GD3 mAb and an anti-PDGFRα antibody. After incubation with an Alexa 568-conjugated anti-mouse IgG antibody and an Alexa 488-conjugated anti-rabbit IgG antibody for secondary antibodies, cells were stained with DAPI to visualize nuclei and observed under a confocal microscopy. The *red color* indicates GD3, and *green* indicates PDGFRα. *Arrowheads* indicate co-localization of GD3 and PDGFRα at the leading edge of cells (*yellow*). *B*, the z-stack image of G(+) cells as in *A*. The image of the *y-z* axis in a *red line* is presented on the *right side of the panel*, and the x-z axis is presented in a *blue line on the bottom side of the panel*. *C*, immunocytochemical staining of G(−) cells and G(+) cells with an anti-Yes antibody and an anti-PDGFRα antibody as described in *A*. Before staining, cells were incubated with DMEM containing 10% FCS for 30 min as described in Fig. 3*E*. *Arrowheads* indicate co-localization of Yes and PDGFRα (*yellow*). *D*, the z-stack image of G(+) cells as in *C*. The *y-z* axis image (*red line*) is presented on the *right side*. The *x-z* axis image (*blue line*) is presented on the *bottom side*. *Scale bars*, 40 μm. *DIC*, differential interference contrast.

In sections of PDGFB-transfected glioma tissues generated in p53-deficient Gtv-a mice, GD3 and/or GD2 and PDGFRα were co-expressed and co-localized exclusively in tumor regions. Moreover, Yes was also co-localized with PDGFRα and was phosphorylated at a high level in PDGFB-transfected glioma tissues (Fig. 7*D*). We also found activated Yes at the edge of PDGFB-transfected glioma tissues (Fig. 8). Although Yes was strongly stained both inside tumor tissues and in surrounding regions, the phosphorylated Yes was stained much stronger at the tumor edge than in the central region of tumor tissues. Actually, GD3, PDGFRα, and Yes were co-localized at tumor edges where Yes was activated. Taken together, these results suggest that GD3 expression might enhance Yes activation by associating with PDGFRα (as shown in Fig. 9), leading to the enhanced invasion activity, particularly in the peripheral regions of glioma tissues.

Discussion

To develop advanced therapy targeting tumor-specific machineries involved in the generation of malignant signals, identification of tumor-specific molecules and elucidation of their roles in the cancer properties are crucial. Tumor-associated ganglioside GD3 is known to be localized in GEM/rafts and generates signals by modulating receptor functions, leading to activation of downstream signaling pathways (35, 36). For example, in human melanoma cells, expression of GD3 up-regulates phosphorylation levels of Akt, p130Cas, FAK, and paxillin after stimulation with fetal calf serum (37). GD3 also enhances adhesion signals by recruiting integrins to GEM/rafts (38). Moreover, GD3 enhances hepatocyte growth factor/Met signals upon cell adhesion to collagen type I (39). Thus, there have been a number of studies reported on the functional aspects of GD3 in melanomas, whereas no studies have been reported to date on the function of GD3 in gliomas.

In this study induction of GD3 in PDGFB-transfected astrocytes was performed, and the properties of PDGFB-induced gliomas were also examined with a focus on the role of GD3 expression. PDGFBB homodimer can bind to all kinds of PDGFR dimers, *i.e.* PDGFRαα, PDGFRαβ, and PDGFRββ, and then trigger PI3K/Akt, RAS/MAPK, and JAK/STAT signals (40). PDGFB signals also induce expression of PDGFRα (41) and form a positive feedback loop between PDGF and PDGFRs to promote oncogenic phenotypes. Interestingly, low or no expression of GD3 could be detected after transfection of cDNA of AKT or KRAS, suggesting that activation of either PI3K/Akt signal or RAS/MAPK signal is insufficient to express GD3, and activation of both of those signals induced by PDGFB is needed to induce definite GD3 expression in astrocytes. Consequently, PDGFRα was identified as a GD3-associated molecule in astrocytes by EMARS and immunoprecipitation-immunoblotting experiments (Fig. 4). Because GD3 stably localizes in GEM/rafts, a part of PDGFRα was reasonably found in GEM/rafts in G(+) cells. These results suggested that GD3 recruits and retains PDGFRα to/in GEM/rafts to form a cluster.

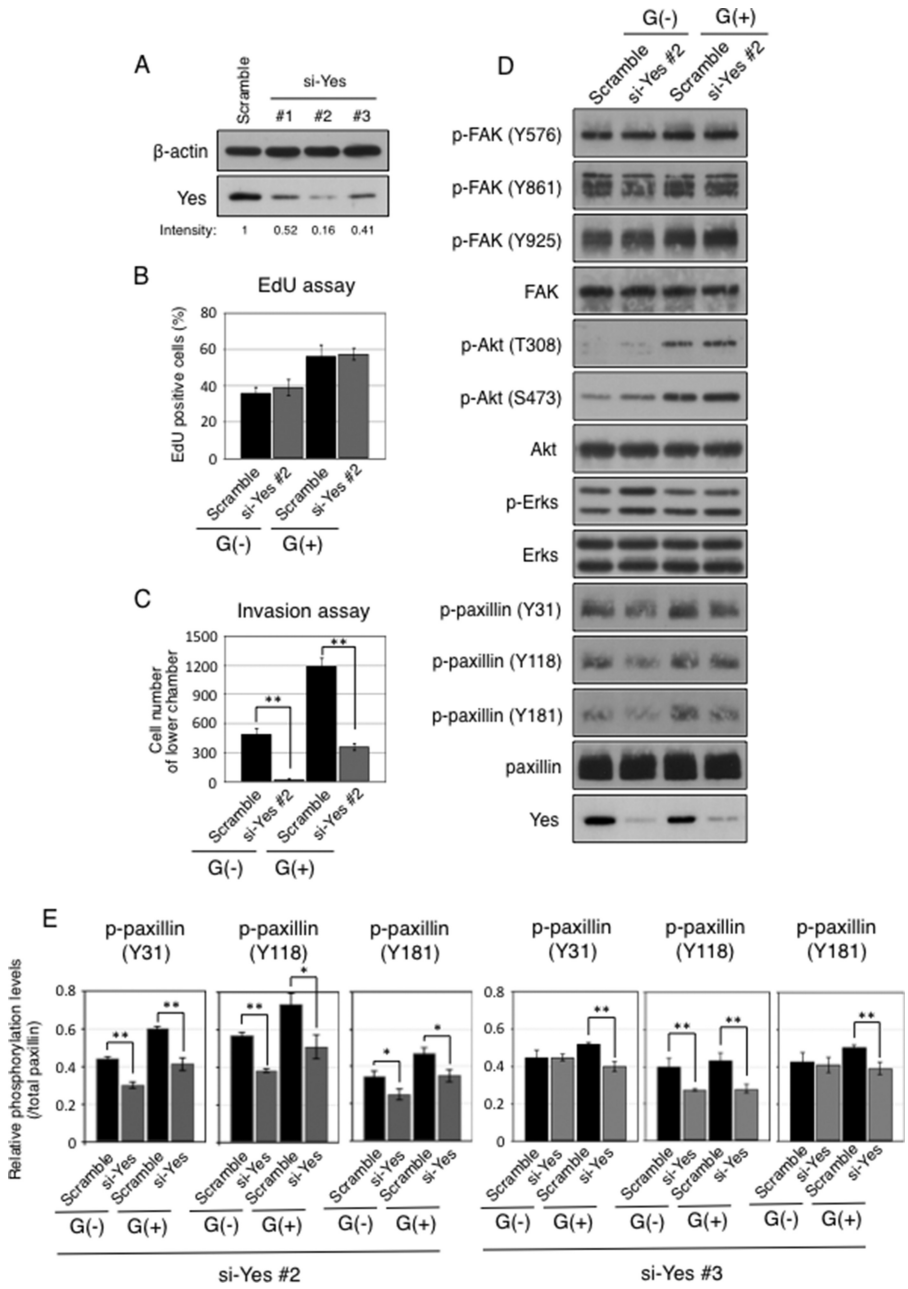

FIGURE 6. **Knockdown of Yes resulted in the attenuation of invasion activities.** *A*, Yes expression levels after 48 h of transfection with three kinds of anti-Yes siRNA (200 pmol) and scramble siRNA in G(+) cells (1×10^6) were examined by Western blotting. Ratios of band intensity of Yes to that of the cells transfected with scramble siRNA were shown. The intensities of bands were measured by using ImageJ software. *B*, EdU uptake in G(+) and G(−) cells after knockdown of Yes. After transfection of siRNA (#2) (200 pmol), cells (1×10^6) were incubated with EdU for 24 h in DMEM containing 0.01% FCS. Staining of incorporated EdU was performed by the manufacturer's protocol. EdU-positive cells were counted at random areas under the fluorescence microscopy. *C*, invasion activities of cells after knockdown of Yes were measured using cell culture inserts. After transfection of siRNA (#2), cells were cultured for 24 h in DMEM containing 10% FCS. Then cells (1×10^3) were re-plated in the upper chambers with serum-free medium. The *lower chamber* was filled with DMEM containing 10% FCS. Invaded cells were counted after incubation for 24 h as described in Fig. 2*D*. *, $p < 0.05$; **, $p < 0.01$. *D*, phosphorylation levels of FAK, Akt, and paxillin in G(+) and G(−) cells after knockdown of Yes (siRNA #2). The lysates were prepared from cells incubated for 24 h in DMEM containing 0.01% FCS after knockdown. Phosphorylation levels of FAK, Akt, ERK, and paxillin were examined by Western blotting using antibodies reactive with individual phosphorylation sites as well as total FAK, Akt, ERK, and paxillin as indicated at the *left side of the bands*. *E*, phosphorylation levels of paxillin in G(−) cells and G(+) cells after knockdown of Yes using siRNAs #2 (200 pmol) or #3 (1 nmol) measured by Image J software. The intensities of phosphorylation levels were normalized with that of paxillin. *, $p < 0.05$; **, $p < 0.01$. *Black bars* indicate cells transfected with scramble siRNA, and *gray bars* with anti-Yes siRNA.

Actually, mechanisms for induction of GD3 expression in this system have not yet been clarified. Transcriptional factor NF-κB has been reported to be one of the regulators for the expression of GD3 synthase gene in human cells (42). Tumor necrosis factor α and interleukin 6 enhanced the expression of GD3 synthase in melanocytes (43), suggesting the involvement of NF-κB. It is also known that there are correlations between NF-κB activation and poor prognosis in gliomas (44). Indeed, high expression of NF-κB RelB proteins promoted glioma cell growth, motility, and invasion *in vitro*, and knockdown of RelB

resulted in the suppression of tumorigenesis *in vivo* (45). Intriguingly, it is reported that RAS/PI3K/Akt/IKK/NF-κB pathway activated by PDGF was associated with anti-apoptotic signaling (46). The elucidation of the mechanisms for up-regulation of GD3 synthase in PDGFB-transfected gliomas remains to be investigated.

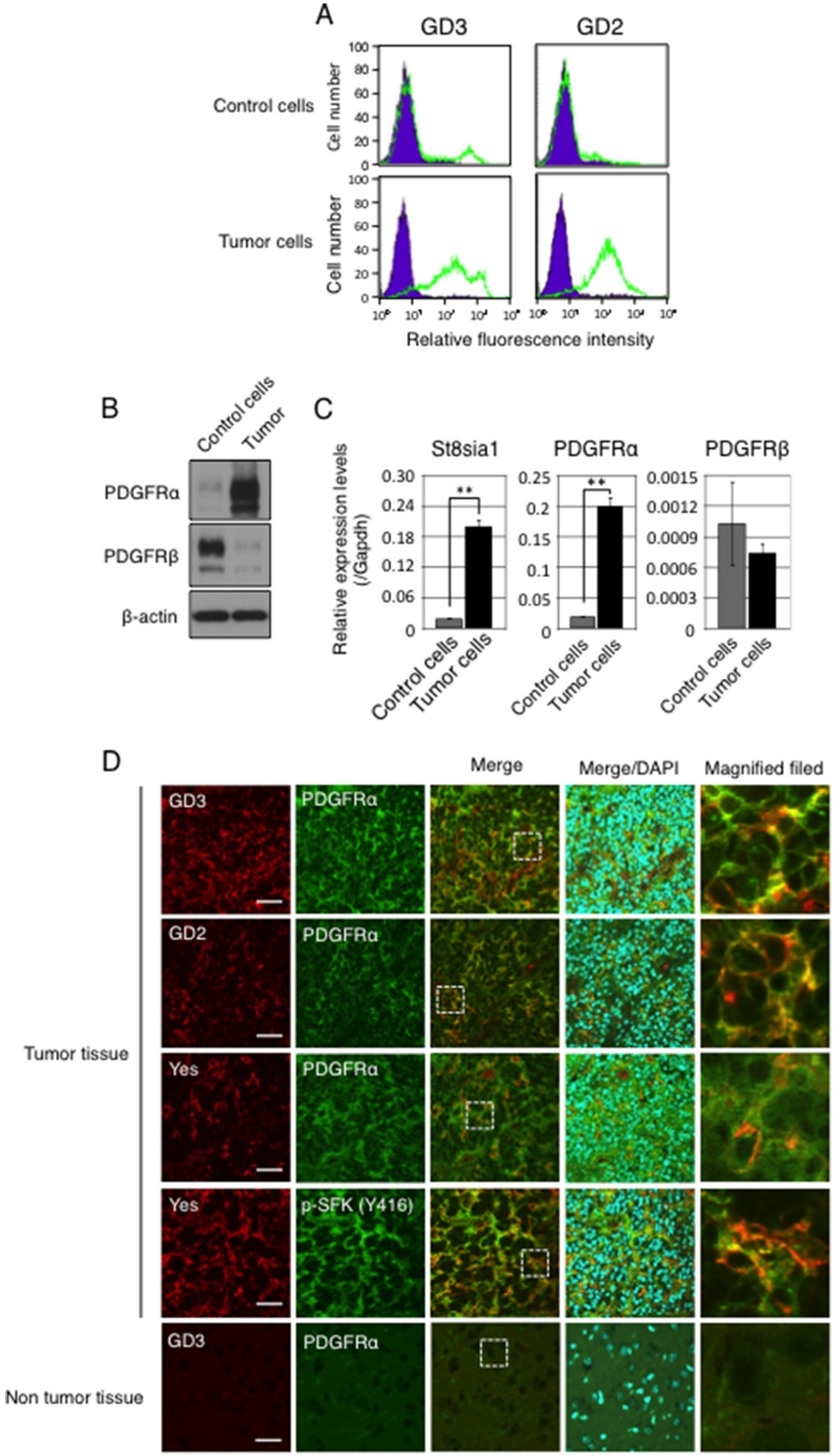

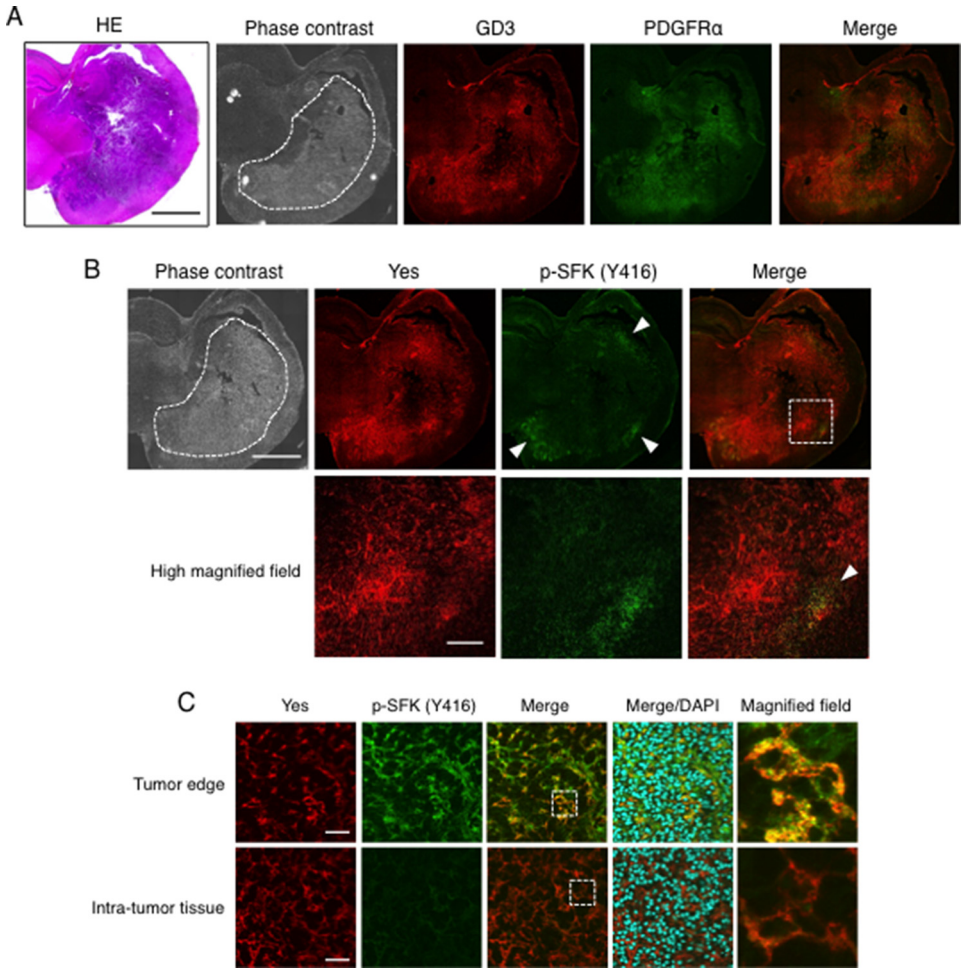

FIGURE 8. **Yes was activated at the invasion front of glioma tissues.** *A*, a coronal section of PDGFB-transfected gliomas generated in a p53$^{-/-}$ Gtv-a mouse at 3 weeks after the transfection was stained with an anti-GD3 mAb (*red*) and an anti-PDGFRα antibody (*green*). The *closed dashed area* represents a location of the tumors in a phase contrast image. *Scale bars*, 2 mm. *B*, sequential sections of PDGFB-transfected glioma tissues as shown in *A*. Double-immunostaining of Yes (*red*) and phosphorylated-Src family kinases (p-SFKs) (*green*) was performed. High-magnified vision fields of the *dashed square region* as indicated in *Merge* were presented in the *lower panels*. The *arrowheads* indicate activated Yes staining at the tumor edge. *Scale bars*, 2 mm (*upper panels*) and 200 μm (*lower panels*). *C*, double-immunostaining of Yes (*red*) and phosphorylated-Src family kinase (*p-SFKs*) (*green*) at the tumor edge, and the intra-tumor tissue was shown. High-magnified fields of dashed square areas as indicated in *Merge* are shown (*right*). *HE*, hematoxylin-eosin. *Scale bars*, 40 μm.

Yes is a non-receptor protein-tyrosine kinase that belongs to Src family kinase proteins. Yes is involved in the regulation of cell growth and survival, apoptosis, cell-cell adhesion, cytoskeleton remodeling, and differentiation (47–49). Kleber *et al.* (50) reported that Yes and the p85 subunit of PI3K are recruited to CD95 by stimulation with CD95 ligand, resulting in an intensive invasion phenotype in glioblastoma multiforme. Our group also reported that GD3 is essential for the functional activation of Yes in human melanoma cells (51). Moreover, the FAK/Src family protein complex activates paxillin via phosphorylation at tyrosine residues 31 and 118 (52). Phosphorylated paxillin promotes the activities of Rho GTPases that enhance invasion activity (53). As shown in Fig. 6, knockdown of Yes in astrocytes dramatically reduced invasion activity by suppressing phosphorylation levels of paxillin in astrocytes, whereas knockdown of Yes did not affect cell proliferation or phosphorylation levels of Akt and ERKs. Together with previous reports, these results suggested that Yes is a key regulator of cell invasion. Intriguingly, almost all Yes was localized in GEM/rafts regardless of GD3 expression in the cells (Fig. 4*D*), showing that the floating pattern of Yes is independent of GD3 expression. These data suggested that GD3 facilitates complex formation between PDGFRα and Yes by recruiting PDGFRα to GEM/rafts. This molecular complex formation seems to be a key event for the

FIGURE 7. **GD3, PDGFRα, and Yes were strongly expressed in PDGFB-transfected gliomas.** *A*, expression levels of GD3 and GD2 in primary cultured glioma cells examined by flow cytometry. After 3 weeks of PDGFB cDNA transfection by RCAS, primary cultured glioma cells were prepared from glioma region of right brain in p53$^{-/-}$ Gtv-a mouse, and control cells were prepared from the normal brain tissue in the opposite side of brain. These experiments were performed within several passages of culture. *B*, expression levels of PDGFRα and PDGFRβ in glioma cells were examined by Western blotting. *C*, mRNA expression levels of St8sia1, PDGFRα, and PDGFRβ in primary cultured glioma cells were examined by quantitative RT-PCR. Expression levels were normalized with Gapdh data. *D*, confocal microscopic images of PDGFB-transfected gliomas generated in a p53$^{-/-}$ Gtv-a mouse. Frozen sections were prepared from brain tissues of p53-deficient Gtv-a mice at 3 weeks after transfection of cDNA of PDGFB by RCAS and were served for double-immunostaining. Co-localizations of GD3 (*red*) and PDGFRα (*green*), GD2 (*red*), and PDGFRα (*green*) and Yes (*red*) and PDGFRα (*green*) in tumor tissues are shown. Double-immunostaining with an anti-Yes antibody and an anti-p-SFK (*Y416*) antibody also showed phosphorylated Yes (*yellow*) in PDGFB-transfected glioma tissues. DAPI (*blue*) was used for nuclear counterstaining. The *right-side images* are high-magnified fields of *dashed square areas* as indicated in *Merge*. *Scale bars*, 40 μm.

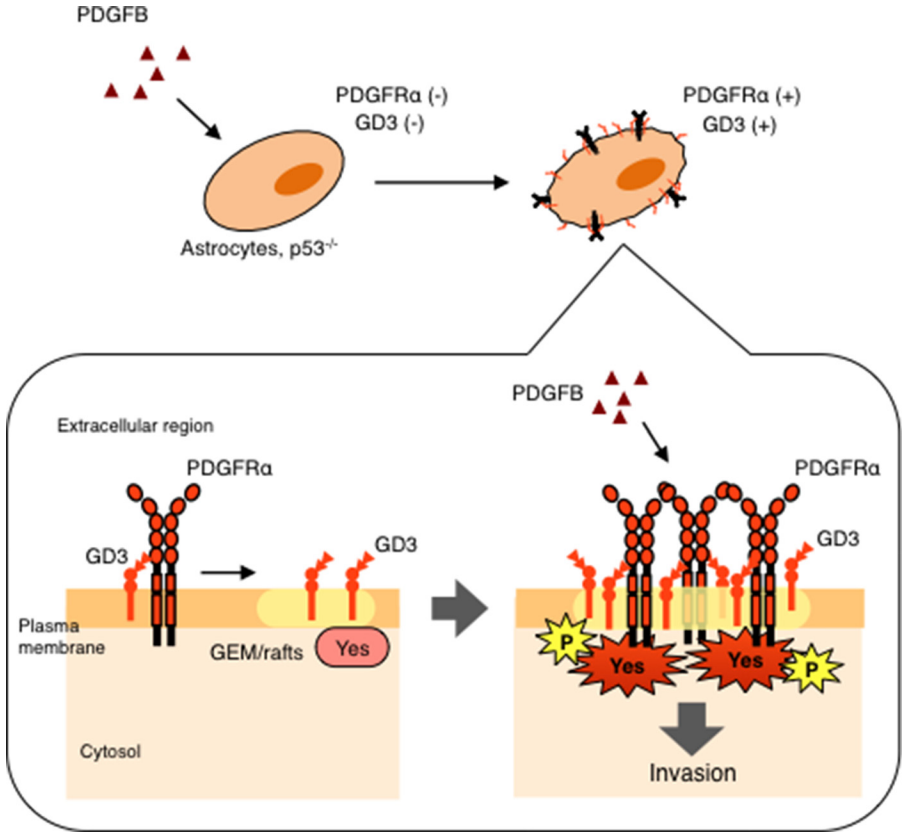

FIGURE 9. **A schema to show roles of GD3 in gliomas.** Expression of GD3 and PDGFRα is induced by PDGFB in p53-deficient astrocytes. GD3 recruits PDGFRα into GEM/rafts, which enhances binding between PDGFRα and Yes kinase. Then PDGFB efficiently activates Yes kinase via PDGFRα, resulting in the increased invasion activity in p53-deficient astrocytes.

activation of a signaling pathway consisting of PDGFRα-Yes-paxillin axis, leading to enhanced invasion activity. Furthermore, the fact that activated Yes, PDGFRα, and GD3 were co-localized at the leading edge of gliomas might be evidence of the importance of PDGFRα-Yes signaling for tumor invasion in gliomas (Fig. 8).

To cure their diseases and their quality of life, glioma patients need to undergo operations and extensive chemotherapeutic and radiation treatments. All treatments of gliomas have the possibility to cause brain dysfunctions. Therefore, novel therapeutic approaches for eradication of glioma cells have been long sought, and the immunological attack of glioma cells with the host defense system might be a promising approach. Tumor-associated carbohydrate antigens including gangliosides are suitable targets for tumor vaccination therapy. In melanomas and small cell lung cancers, challenges of antibody therapy trials have been performed using anti-GD3 mAbs (54). GD2 has also been used as a target of antibody therapy in human neuroblastomas (55). MHC-independent chimeric antigen receptors directed to GD2 has been generated and tested in neuroblastoma cells and patients (56). GD2-CAR T cells could induce complete tumor responses in patients with active neuroblastomas (57). In addition, GD2 was characterized as a maker of cancer stem cells in breast cancer, indicating that GD2-targeted therapy might eliminate cancer stem cells (58). Our findings that GD3 and/or GD2 are specifically expressed in glioma tissues in adult brain and play roles in the modulation of PDGFRα/Yes/paxillin signaling, leading to the increased invasion, provide approaches for the development of novel therapeutics targeting there gangliosides for glioma patient.

Acknowledgments—We thank T. Mizuno, Y. Nakayasu, and H. Takei for technical assistance. We acknowledge the Division for Medical Research Engineering, Nagoya University Graduate School of Medicine, M. Tanaka for technical support of FACS Aria II™, and K. Taki for technical support of mass spectrometry analysis by LTQ Orbitrap XL™.

References

1. Daniotti, J. L., Vilcaes, A. A., Torres Demichelis, V., Ruggiero, F. M., and Rodriguez-Walker, M. (2013) Glycosylation of glycolipids in cancer: basis for development of novel therapeutic approaches. *Front. Oncol.* **3,** 306
2. Hakomori, S. (2004) Glycosynapses: microdomains controlling carbohydrate-dependent cell adhesion and signaling. *An. Acad. Bras. Cienc.* **76,** 553–572
3. Ohmi, Y., Tajima, O., Ohkawa, Y., Yamauchi, Y., Sugiura, Y., and Furukawa, K. (2011) Gangliosides are essential in the protection of inflammation and neurodegeneration via maintenance of lipid rafts: elucidation by a series of ganglioside-deficient mutant mice. *J. Neurochem.* **116,** 926–935
4. Vajn, K., Viljetić, B., Degmečić, I. V., Schnaar, R. L., and Heffer, M. (2013) Differential distribution of major brain gangliosides in the adult mouse central nervous system. *PLoS ONE* **8,** e75720
5. Yu, R. K., Nakatani, Y., and Yanagisawa, M. (2009) The role of glycosphingolipid metabolism in the developing brain. *J. Lipid Res.* **50,** S440–S445
6. Yamashiro, S., Okada, M., Haraguchi, M., Furukawa, K., Lloyd, K. O., and Shiku, H. (1995) Expression of α-2,8-sialyltransferase (GD3 synthase) gene in human cancer cell lines: high level expression in melanomas and up-regulation in activated T lymphocytes. *Glycoconj. J.* **12,** 894–900

7. Okada, M., Furukawa, K., Yamashiro, S., Yamada, Y., Haraguchi, M., Horibe, K., Kato, K., and Tsuji, Y. (1996) High expression of ganglioside α-2,8-sialyltransferase (GD3 synthase) gene in adult T-cell leukemia cells unrelated to the gene expression of human T-lymphotropic virus type I. *Cancer Res.* **56,** 2844–2848
8. Wagener, R., Röhn, G., Schillinger, G., Schröder, R., Kobbe, B., and Ernestus, R. I. (1999) Ganglioside profiles in human gliomas: quantification by microbore high performance liquid chromatography and correlation to histomorphology and grading. *Acta Neurochir.* **141,** 1339–1345
9. Vukelić, Z., Kalanj-Bognar, S., Froesch, M., Bîndila, L., Radić, B., Allen, M., Peter-Katalinić, J., and Zamfir, A. D. (2007) Human gliosarcoma-associated ganglioside composition is complex and distinctive as evidenced by high-performance mass spectrometric determination and structural characterization. *Glycobiology* **17,** 504–515
10. Furnari, F. B., Fenton, T., Bachoo, R. M., Mukasa, A., Stommel, J. M., Stegh, A., Hahn, W. C., Ligon, K. L., Louis, D. N., Brennan, C., Chin, L., DePinho, R. A., and Cavenee, W. K. (2007) Malignant astrocytic glioma: genetics, biology, and paths to treatment. *Genes Dev.* **21,** 2683–2710
11. Wen, P. Y., and Kesari, S. (2008) Malignant gliomas in adults. *N. Engl. J. Med.* **359,** 492–507
12. Cancer Genome Atlas Research Network. (2008) Comprehensive genomic characterization defines human glioblastoma genes and core pathways. *Nature* **455,** 1061–1068
13. Verhaak, R. G., Hoadley, K. A., Purdom, E., Wang, V., Qi, Y., Wilkerson, M. D., Miller, C. R., Ding, L., Golub, T., Mesirov, J. P., Alexe, G., Lawrence, M., O'Kelly, M., Tamayo, P., Weir, B. A., Gabriel, S., Winckler, W., Gupta, S., Jakkula, L., Feiler, H. S., Hodgson, J. G., James, C. D., Sarkaria, J. N., Brennan, C., Kahn, A., Spellman, P. T., Wilson, R. K., Speed, T. P., Gray, J. W., Meyerson, M., Getz, G., Perou, C. M., Hayes, D. N., and Cancer Genome Atlas Research Network (2010) Integrated genomic analysis identifies clinically relevant subtypes of glioblastoma characterized by abnormalities in PDGFRA, IDH1, EGFR, and NF1. *Cancer Cell* **17,** 98–110
14. Brennan, C., Momota, H., Hambardzumyan, D., Ozawa, T., Tandon, A., Pedraza, A., and Holland E. (2009) Glioblastoma subclasses can be defined by activity among signal transduction pathways and associated genomic alterations. *PLoS ONE* **4,** e7752
15. Zhu, H., Acquaviva, J., Ramachandran, P., Boskovitz, A., Woolfenden, S., Pfannl, R., Bronson, R. T., Chen, J. W., Weissleder, R., Housman, D. E., and Charest, A. (2009) Oncogenic EGFR signaling cooperates with loss of tumor suppressor gene functions in gliomagenesis. *Proc. Natl. Acad. Sci. U.S.A.* **106,** 2712–2716
16. MacDonald, T. J., Brown, K. M., LaFleur, B., Peterson, K., Lawlor, C., Chen, Y., Packer, R. J., Cogen, P., and Stephan, D. A. (2001) Expression profiling of medulloblastoma: PDGFRA and the RAS/MAPK pathway as therapeutic targets for metastatic disease. *Nat. Genet.* **29,** 143–152
17. Demuth, T., and Berens, M. E. (2004) Molecular mechanisms of glioma cell migration and invasion. *J. Neurooncol.* **70,** 217–228
18. Momota, H., Narita, Y., Matsushita, Y., Miyakita, Y., and Shibui, S. (2010) p53 abnormality and tumor invasion in patients with malignant astrocytoma. *Brain Tumor Pathol.* **27,** 95–101
19. Heyer, J., Kwong, L. N., Lowe, S. W., and Chin, L. (2010) Non-germline genetically engineered mouse models for translational cancer research. *Nat. Rev. Cancer* **10,** 470–480
20. Hambardzumyan, D., Amankulor, N. M., Helmy, K. Y., Becher, O. J., and Holland, E. C. (2009) Modeling adult gliomas using RCAS/t-va technology. *Transl. Oncol.* **2,** 89–95
21. Holland, E. C., and Varmus, H. E. (1998) Basic fibroblast growth factor induces cell migration and proliferation after glia-specific gene transfer in mice. *Proc. Natl. Acad. Sci. U.S.A.* **95,** 1218–1223
22. Holland, E. C., Celestino, J., Dai, C., Schaefer, L., Sawaya, R. E., and Fuller, G. N. (2000) Combined activation of Ras and Akt in neural progenitors induces glioblastoma formation in mice. *Nat. Genet.* **25,** 55–57
23. Holland, E. C., Hively, W. P., DePinho, R. A., and Varmus, H. E. (1998) A constitutively active epidermal growth factor receptor cooperates with disruption of G_1 cell-cycle arrest pathways to induce glioma-like lesions in mice. *Genes Dev.* **12,** 3675–3685
24. Suzumura, A., Sawada, M., and Marunouchi, T. (1996) Selective induction of interleukin-6 mouse microglia by granulocyte-macrophage colony-stimulating factor. *Brain Res.* **713,** 192–198
25. Suzumura, A., Mezitis, S. G., Gonatas, N. K., and Silberberg, D. H. (1987) MHC antigen expression on bulk isolated macrophage-microglia from newborn mouse brain: induction of Ia antigen expression by γ-interferon. *J. Neuroimmunol.* **15,** 263–278
26. Zhao, J., Furukawa, K., Fukumoto, S., Okada, M., Furugen, R., Miyazaki, H., Takamiya, K., Aizawa, S., Shiku, H., Matsuyama, T., and Furukawa, K. (1999) Attenuation of interleukin 2 signal in the spleen cells of complex ganglioside-lacking mice. *J. Biol. Chem.* **274,** 13744–13747
27. Hashimoto, N., Hamamura, K., Kotani, N., Furukawa, K., Kaneko, K., and Honke, K. (2012) Proteomic analysis of ganglioside-associated membrane molecules: substantial basis for molecular clustering. *Proteomics* **12,** 3154–3163
28. Eddleston, M., and Mucke, L. (1993) Molecular profile of reactive astrocytes: implications for their role in neurologic disease. *Neuroscience* **54,** 15–36
29. Kawai, K., Kuroda, S., Watarai, S., Takahashi, H., and Ikuta, F. (1994) Occurrence of GD3 gangliosides in reactive astrocytes: an immunocytochemical study in the rat bain. *Neurosci. Lett.* **174,** 225–227
30. Kawai, K., Watarai, S., Takahashi, H., Ishizu, H., Fukai, K., Tanabe, Y., Yokota, O., and Kuroda, S. (1999) Demonstration of ganglioside GD3 in human reactive astrocytes. *Psychiatry Clin. Neurosci.* **53,** 79–82
31. Zamanian, J. L., Xu, L., Foo, L. C., Nouri, N., Zhou, L., Giffard, R. G., and Barres, B. A. (2012) Genomic analysis of reactive astrogliosis. *J. Neurosci.* **32,** 6391–6410
32. Furukawa, K., Ohmi, Y., Ohkawa, Y., Tokuda, N., Kondo, Y., Tajima, O., and Furukawa, K. (2011) Regulatory mechanisms of nervous systems with glycosphingolipids. *Neurochem. Res.* **36,** 1578–1586
33. Kotani, N., Gu, J., Isaji, T., Udaka, K., Taniguchi, N., and Honke, K. (2008) Biochemical visualization of cell surface molecular clustering in living cells. *Proc. Natl. Acad. Sci. U.S.A.* **105,** 7405–7409
34. Deakin, N. O., Pignatelli, J., and Turner, C. E. (2012) Diverse roles for the paxillin family of proteins in cancer. *Genes Cancer* **3,** 362–370
35. Furukawa, K., Hamamura, K., Ohkawa, Y., and Ohmi, Y. (2012) Disialyl gangliosides enhance tumor phenotypes with differential modalities. *Glycoconj. J.* **29,** 579–584
36. Furukawa, K., Ohkawa, Y., Yamauchi, Y., Hamamura, K., and Ohmi, Y. (2012) Fine tuning of cell signals by glycosylation. *J. Biochem.* **151,** 573–578
37. Hamamura, K., Furukawa, K., Hayashi, T., Hattori, T., Nakano, J., Nakashima, H., Okuda, T., Mizutani, H., Hattori, H., Ueda, M., Urano, T., and Lloyd, K. O. (2005) Ganglioside GD3 promotes cell growth and invasion through p130Cas and paxillin in malignant melanoma cells. *Proc. Natl. Acad. Sci. U.S.A.* **102,** 11041–11046
38. Ohkawa, Y., Miyazaki, S., Hamamura, K., Kambe, M., Miyata, M., Tajima, O., Ohmi, Y., Yamauchi, Y., and Furukawa, K. (2010) Ganglioside GD3 enhances adhesion signals and augments malignant properties of melanoma cells by recruiting integrins to glycolipid-enriched microdomains. *J. Biol. Chem.* **285,** 27213–27223
39. Furukawa, K., Kambe, M., Miyata, M., Ohkawa, Y., Tajima, O., and Furukawa, K. (2014) Ganglioside GD3 induces convergence and synergism of adhesion and hepatocyte growth factor/Met signals in melanomas. *Cancer Sci.* **105,** 52–63
40. Shih, A. H., and Holland, E. C. (2006) Platelet-derived growth factor (PDGF) and glial tumorigenesis. *Cancer Lett.* **232,** 139–147
41. Dai, C., Celestino, J. C., Okada, Y., Louis, D. N., Fuller, G. N., and Holland, E. C. (2001) PDGF autocrine stimulation dedifferentiates cultured astrocytes and induces oligodendrogliomas and oligoastrocytomas from neural progenitors and astrocytes *in vivo*. *Genes Dev.* **15,** 1913–1925
42. Kang, N. Y., Kim, C. H., Kim, K. S., Ko, J. H., Lee, J. H., Jeong, Y. K., and Lee, Y. C. (2007) Expression of the human CMP-NeuAc:GM3 α2,8-sialyltransferase (GD3 synthase) gene through the NF-κB activation in human melanoma SK-MEL-2 cells. *Biochim. Biophys. Acta* **1769,** 622–630
43. Miyata, M., Ichihara, M., Tajima, O., Sobue, S., Kambe, M., Sugiura, K., and Furukawa, K. (2014) UVB-irradiated keratinocytes induce melanoma-associated ganglioside GD3 synthase gene in melanocytes via secretion of tumor necrosis factor α and interleukin 6. *Biochem. Biophys. Res. Commun.* **445,** 504–510

44. Park, S., Hatanpaa, K. J., Xie, Y., Mickey, B. E., Madden, C. J., Raisanen, J. M., Ramnarain, D. B., Xiao, G., Saha, D., Boothman, D. A., Zhao, D., Bachoo, R. M., Pieper, R. O., and Habib, A. A. (2009) The receptor interacting protein 1 inhibits p53 induction through NF-κB activation and confers a worse prognosis in glioblastoma. *Cancer Res.* **69,** 2809–2816
45. Lee, D. W., Ramakrishnan, D., Valenta, J., Parney, I. F., Bayless, K. J., and Sitcheran, R. (2013) The NF-κB RelB protein is an oncogenic driver of mesenchymal glioma. *PLoS ONE* **8,** e57489
46. Romashkova, J. A., and Makarov, S. S. (1999) NF-κB is a target of AKT in anti-apoptotic PDGF signalling. *Nature* **401,** 86–90
47. Thomas, S. M., and Brugge, J. S. (1997) Cellular functions regulated by Src family kinases. *Annu. Rev. Cell Dev. Biol.* **13,** 513–609
48. Jung, J., Lee, M. K., Jin, Y., Fu, S. B., Rosales, J. L., and Lee, K. Y. (2011) Clues for c-Yes involvement in the cell cycle and cytokinesis. *Cell Cycle* **10,** 1502–1503
49. Sato, A., Sekine, M., Virgona, N., Ota, M., and Yano, T. (2012) Yes is a central mediator of cell growth in malignant mesothelioma cells. *Oncol. Rep.* **28,** 1889–1893
50. Kleber, S., Sancho-Martinez, I., Wiestler, B., Beisel, A., Gieffers, C., Hill, O., Thiemann, M., Mueller, W., Sykora, J., Kuhn, A., Schreglmann, N., Letellier, E., Zuliani, C., Klussmann, S., Teodorczyk, M., Gröne, H. J., Ganten, T. M., Sültmann, H., Tüttenberg, J., von Deimling, A., Regnier-Vigouroux, A., Herold-Mende, C., and Martin-Villalba, A. (2008) Yes and PI3K bind CD95 to signal invasion of glioblastoma. *Cancer Cell* **13,** 235–248
51. Hamamura, K., Tsuji, M., Hotta, H., Ohkawa, Y., Takahashi, M., Shibuya, H., Nakashima, H., Yamauchi, Y., Hashimoto, N., Hattori, H., Ueda, M., and Furukawa, K. (2011) Functional activation of Src family kinase yes protein is essential for the enhanced malignant properties of human melanoma cells expressing ganglioside GD3. *J. Biol. Chem.* **286,** 18526–18537
52. Schaller, M. D., and Parsons, J. T. (1995) pp125FAK-dependent tyrosine phosphorylation of paxillin creates a high-affinity binding site for Crk. *Mol. Cell Biol.* **15,** 2635–2645
53. Deakin, N. O., and Turner, C. E. (2011) Distinct roles for paxillin and Hic-5 in regulating breast cancer cell morphology, invasion and metastasis. *Mol. Biol. Cell* **22,** 327–341
54. Heimburg-Molinaro, J., Lum, M., Vijay, G., Jain, M., Almogren, A., and Rittenhouse-Olson, K. (2011) Cancer vaccines and carbohydrate epitopes. *Vaccine* **29,** 8802–8826
55. Yang, R. K., and Sondel, P. M. (2010) Anti-GD2 strategy in the treatment of neuroblastoma. *Drugs Future* **35,** 665
56. Pule, M. A., Savoldo, B., Myers, G. D., Rossig, C., Russell, H. V., Dotti, G., Huls, M. H., Liu, E., Gee, A. P., Mei, Z., Yvon, E., Weiss, H. L., Liu, H., Rooney, C. M., Heslop, H. E., and Brenner, M. K. (2008) Virus-specific T cells engineered to coexpress tumor-specific receptors: persistence and antitumor activity in individuals with neuroblastoma. *Nat. Med.* **14,** 1264–1270
57. Louis, C. U., Savoldo, B., Dotti, G., Pule, M., Yvon, E., Myers, G. D., Rossig, C., Russell, H. V., Diouf, O., Liu, E., Liu, H., Wu, M. F., Gee, A. P., Mei, Z., Rooney, C. M., Heslop, H. E., and Brenner, M. K. (2011) Antitumor activity and long-term fate of chimeric antigen receptor-positive T cells in patients with neuroblastoma. *Blood* **118,** 6050–6056
58. Battula, V. L., Shi, Y., Evans, K. W., Wang, R. Y., Spaeth, E. L., Jacamo, R. O., Guerra, R., Sahin, A. A., Marini, F. C., Hortobagyi, G., Mani, S. A., and Andreeff, M. (2012) Ganglioside GD2 identifies breast cancer stem cells and promotes tumorigenesis. *J. Clin. Invest.* **122,** 2066–2078